Presented at Synchrotron Radiation Instrumentation 1995
Chicago, IL, October 15-20, 1995

BNL-64133
CONF-9510119--41

A review of methods for experimentally determining linear optics in storage rings*

J. Safranek
National Synchrotron Light Source, Brookhaven National Laboratory, Upton, NY 11973

Abstract

In order to maximize the brightness and provide sufficient dynamic aperture in synchrotron radiation storage rings, one must understand and control the linear optics. Control of the horizontal beta function and dispersion is important for minimizing the horizontal beam size. Control of the skew gradient distribution is important for minimizing the vertical size. In this paper, various methods for experimentally determining the optics in a storage ring will be reviewed. Recent work at the National Synchrotron Light Source X-Ray Ring will be presented as well as work done at laboratories worldwide.

I. Introduction

The measured optics of a storage ring never completely agree with the predictions of computer models of the storage ring design. Traditionally, accelerator physicists have measured the horizontal and vertical betatron tunes and the beta functions at the quadrupoles, and then adjusted a subset of the many parameters of the computer model to make the model electron optics better fit the measurements. There was no certainty that the correct parameters were adjusted to achieve this improved fit. The optimized model fit the measurements better, but did not necessarily give the true lattice of the storage ring.

This paper will review some recent work that has been done to better understand electron storage ring optics by using measured orbit data. The goal of the paper is to provide an overview of recent work not a comprehensive survey. Improvements in orbit measurement hardware including beam position monitors (BPMs) that measure the closed orbit to micron precision, fast digitizers capable of storing many turns of single turn orbit measurements, and computers capable of analyzing the large amount of data generated make these methods of analyzing accelerator optics practical.

Turn-by-turn betatron oscillations ($x_{b,n}$) about the closed orbit measured at some BPM,

$$x_{b,n} = a\sqrt{\beta_b}\cos(2\pi n\nu + \phi_b), \qquad (1)$$

can be determined by the betatron function and phase [1] at the BPM (β_b, ϕ_b), as well as the betatron phase for the whole ring ($2\pi\nu$). The integer n increases by unity for each revolution of the electron bunch, and a is the initial amplitude. In this paper, work will be described in which a harmonic analysis of many turns of $x_{b,n}$ is taken to yield the betatron function and phase at the BPMs.[4], [5], [7], [8]

The shift in closed orbit at a BPM ($x_{b,c.o.}$) from changing one of the orbit steering magnets by angle θ also depends only on the betatron function and phase,

$$x_{b,c.o.} = \theta\frac{\sqrt{\beta_b\beta_s}}{2\sin\pi\nu}\cos(|\phi_b - \phi_s| - \pi\nu), \qquad (2)$$

where (β_s, ϕ_s) are the beta function and phase at the steering magnet. Work will be described in which this equation is inverted to give the beta function and phase at the BPMs and steering magnets.[10], [14]

Another approach is to determine the actual individual magnet field gradients from orbit measurements.[11], [12], [13], [15], [17], [16] The beta functions and phases are determined by the magnetic gradient distribution in the storage ring ($K(s)$),

$$\frac{1}{2}\beta\beta'' - \frac{1}{4}\beta + K\beta^2 = 1, \qquad (3)$$

$$\phi' = \frac{1}{\beta}. \qquad (4)$$

The derivatives are with respect to longitudinal position in the ring, s. Through equations 1, 2, 3, and 4, orbit shifts and orbit oscillations at the BPMs are determined by the gradients in the quadrupoles. It is possible to invert this set of equations, and determine the gradients from orbit measurements. Once the magnetic field gradients are derived, the beta functions and phases are determined everywhere in the ring, not just at the BPMs and steering magnets.

II. Turn-by-turn orbit data

A. *First turns at APS*

When commissioning a storage ring, single pass orbit measurements for the first turn or first few turns have proven useful for diagnosing major magnet gradient errors.[11], [2], [3] Figure 1 shows an example of the shift in the first turn orbit with a steering magnet measured during commissioning of the APS. Despite the relatively large error in measuring the orbit with the small single-pulse current during injection, comparison of the measured orbit shift to that of a fit with the computer model shows an obvious large gradient error. This error was subsequently confirmed when one of the quadrupoles was found to be mistakenly connected to a sextupole power supply.

*Work performed under the auspices of the U.S. Department of Energy

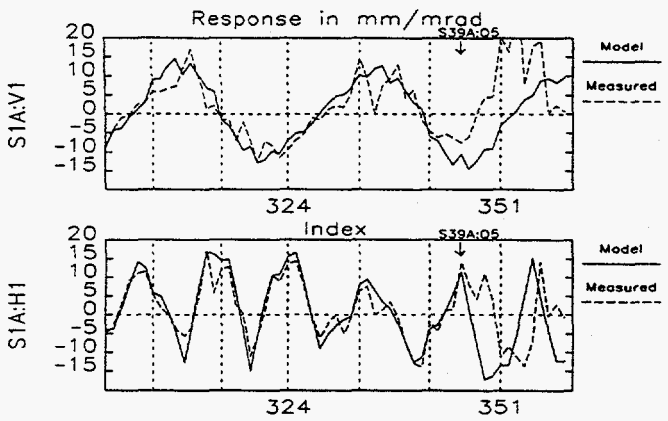

Figure. 1. The vertical (upper plot) and horizontal (lower plot) shifts in the first turn orbit in APS with orbit steerer S1A:HV1 shows gradient error in quadrupole S39A:Q5.

Once the major gradient errors are eliminated and larger single-bunch currents can be stored, harmonic analysis of turn-by-turn betatron oscillations over hundreds or thousands of turns gives the relative betatron functions and phases at the BPMs (β_b and ϕ_b in equation 2). The first such work was performed at SSRL [4], [5], and was a direct development of previous work using network analyzers (see, for example [6]).

B. Multi-turn digitization at LEP

The most extensive application of this method has been performed at CERN [7], [8], where hardware capable of simultaneously digitizing 1024 consecutive turns at 504 BPMs has been implemented on the LEP storage ring. The amplitude of the measured oscillation at each BPM depends on β_b and the gain of the BPM, which is not well known, so simply looking at the measured amplitude does not give an accurate measure of β_b. The phase of the oscillation, however, is independent of the BPM gain calibrations, so the betatron phases, ϕ_b, can be measured quite accurately. The beta function is the inverse of the derivative of the betatron phase (equation 4), so the measured betatron phases can be used to determine the beta function. To do this, the measured phases were fit to a function with the following form,

$$\phi(s) = \phi_0(s) + B(s)\sin\left[2\phi_0(s) + \lambda(s)\right] + d(s), \qquad (5)$$

where $\phi_0(s)$ is the phase according to the MAD[9] computer model and the functions $B(s)$, $\lambda(s)$ and $d(s)$ are slowly varying functions. An oscillation of this form in the measured phase with respect to the model phase is to be expected from small gradient errors in the quadrupoles (see, for example [1]). The values of $B(s)$, $\lambda(s)$ and $d(s)$ were assumed to be constant over small sections of the ring, and were determined by fitting $\phi(s)$ to ϕ_b over each section. Then the derivative of $\phi(s)$ was taken to determine $\beta(s)$. The 20% peak-to-peak beat in the beta function in LEP was thus accurately measured. $\beta(s)$ also gives a value of β_b for each BPM which, with the measured oscillation amplitude at each BPM, could be used to calibrate the BPM gain.

III. Closed orbit data

Two common ways of measuring machine optics using closed orbit shifts are to look at the shift in closed orbit from single steering magnets (see, for example [10], [11], [12], [13], [14], [15], [16]) or to make local orbit bumps using combinations of steering magnets[17].

A. Orbit bumps in Tristan

The work at Tristan[17] is the first of two methods I will describe in which the actual gradients of the storage ring magnets were experimentally determined. Figure 2 shows schematically the algorithm used to determine the Tristan optics.

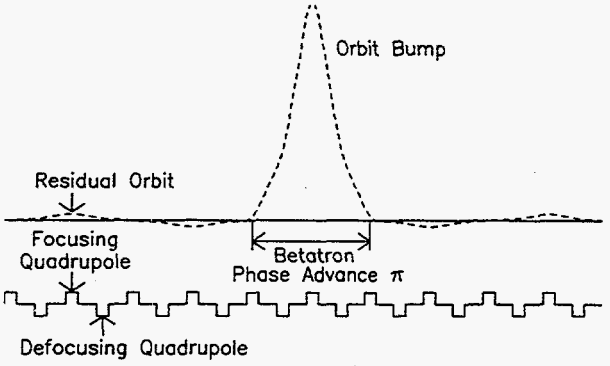

Figure. 2. Measurement of quadrupole gradient error using an orbit bump with betatron phase advance of π.

The magnet structure in Tristan is FODO, which is a periodic structure in which each cell has one focusing and one defocusing quadrupole. During the experiment, the optics were adjusted to give $\pi/2$ betatron phase advance per cell. Equal dipole steering kicks were given next to two quadrupoles, separated by π in phase advance. This should have resulted in a purely local closed orbit distortion. Therefore, the residual orbit distortion around the ring was due to errors in the quadrupole gradients inside the local bump or to errors in the calibration of the dipole kicks used to make the bump. By analyzing the residual orbits from all the different π bumps, the quadrupole gradient errors (both normal and skew) could be derived. Also, using the same bumps but with the sextupoles turned on inside the bumps, the horizontal and vertical offsets of the electron beam from the center of each sextupole could be determined. In this way, the gradients in Tristan were determined to very high precision. Using the improved understanding of the linear optics, the measured dynamic aperture in Tristan was predicted by the model with an unprecedented accuracy.

The experiment at Tristan was simplified by the fact that the optics were set up to give π phase advance between steering kicks, so only two steering kicks were necessary to

DISCLAIMER

make a local bump. In addition, the quadrupole at the center of the bump was approximately $\pi/2$ in phase advance from the two steering kicks, so the residual orbit from gradient errors in the quadrupoles were easy to distinguish from residual orbit distortion caused by calibration errors in the steering kicks. It is unclear whether the local bump method could be applied in storage rings designed for synchrotron radiation, where, in general, three orbit kicks are required for a local bump and the quadrupoles are not $\pi/2$ in phase advance from the orbit steering magnets.

B. Orbit response matrix analysis

Equation 1 gives a representation of the orbit response matrix which is the change in orbit at every BPM for a change in strength of every steering magnet. In reference [14] a method is presented for inverting this equation to derive the beta functions and phase advances at the BPMs and steering magnets from the measured orbit response matrix. Just as with the analysis of free betatron oscillations at LEP, the analysis of the measured orbit response matrix gives a very accurate measurement of betatron phase advance, but the accuracy of the fit beta functions is limited by errors in the calibration of the BPMs and steering magnets. The beta function, however, can be derived from the fit phase advances, as was done at LEP.

In reference [16] another method of analyzing the measured response matrix data is presented in which the quadrupole gradients are derived. The gradients in a MAD[9] model of the NSLS X-Ray Ring were varied in order to minimize the χ^2 deviation between the model and the measured orbit response matrices (M_{mod} and M_{meas}).

$$\chi^2 = \sum_{i,j} \frac{(M_{mod,ij} - M_{meas,ij})^2}{\sigma_i^2}, \qquad (6)$$

where the double sum is taken over the orbit steering magnets and the BPMs. The σ_i are the measured noise levels for the BPMs. The matrices include the coupling terms (i.e. vertical orbit shifts with horizontal steering magnets and horizontal orbit shifts with vertical steering). With this method the normal and skew gradients in each individual quadrupole can be determined. These gradients, in turn, define the beta functions and betatron phases throughout the ring, not just at the BPMs and orbit steering magnets. This algorithm also yields the calibrations and rotations of the BPMs and steering magnets. For those quadrupoles adjacent to sextupoles, the analysis was not able to differentiate well between gradient errors in the quadrupoles and sextupole gradients due to orbit offsets from the sextupole magnetic centers. This problem was solved by first measuring the orbit response matrix with the sextupoles off, and then measuring the matrix with the sextupoles on. The first matrix was used to calibrate the gradients in the quadrupoles, and the second matrix was used to find the gradient in the sextupoles.

Once the model was fit to the measurements to minimize χ^2, the RMS difference between the model and the measured response matrices was only 1.2 μm which is primarily due to random noise in the orbit measurements. The noise propagated to give very small error bars on the fit parameters and beta functions as shown in table 1. The small error bars are a direct result of the high precision of the BPM system at NSLS.[18]

Table 1. These RMS variations are the error bars on the fit parameters due to random orbit measurement errors.

Parameter	RMS variation
quadrupole gradients	.04 %
quadrupole rotations	.4 mrad
BPM gain	.5 %
BPM rotations	.5 mrad
steering magnet calibration	.5 %
steering magnet rotations	.8 mrad
beta functions	.08 %

Tests were performed to confirm that this algorithm could resolve small changes in the quadrupole gradients. Figure 3 shows the results of one such test. For this test the response matrix was measured. Then the gradients in two of the four families of quadrupole in the X-Ray Ring were changed, and the response matrix was measured again. Each response matrix was analyzed separately, and comparison of the two sets of fit parameters showed that the algorithm did an excellent job of correctly resolving the changes in the quadrupole gradients.

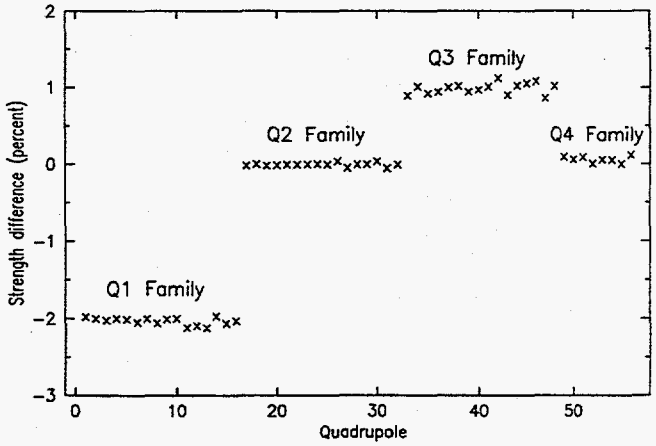

Figure. 3. This plot shows the ratio of the fit gradients for the 56 quadrupoles in the X-Ray Ring before and after changing the Q1 and Q4 quadrupole family gradients. The fitting algorithm successfully resolved the changes made in the quadrupole gradients.

The fit parameters that were independently measured agreed with the results from the χ^2 fitting. For example, figure 4 shows the excellent agreement between the fit BPM rotations and the BPM rotations physically measured in the X-Ray Ring. Also, other measured optics parameters that were not used in the χ^2 fitting confirmed that the fit model is correct. For example, figure 5 shows the agreement between the measured dispersion and the dispersion predicted by the fit model.

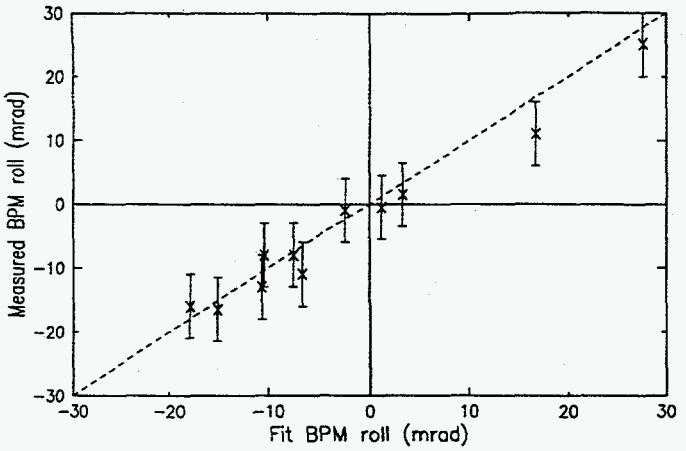

Figure. 4. This plot compares several of the BPM rotations found by fitting the orbit response matrix to those rotations found by measuring the actual BPM alignment. The fit values agree with the measured values to within the error bars of the measurement.

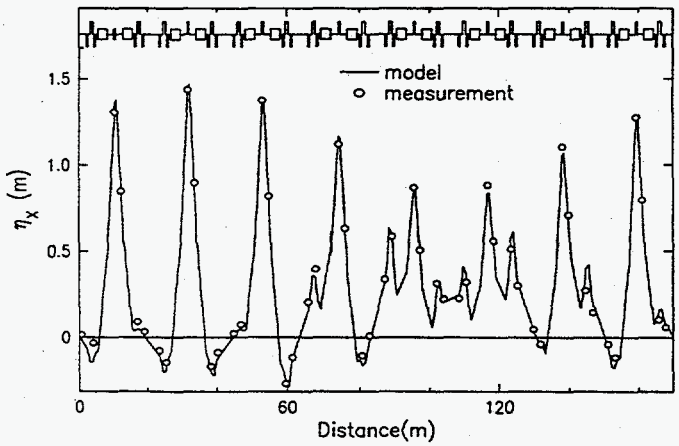

Figure. 5. The dispersion function distortions in the X-Ray Ring are due to gradient errors, primarily from orbit offsets in sextupoles. The fit model agrees well with the measured dispersion.

The improved knowledge of the X-Ray Ring optics achieved through the orbit response matrix analysis has provided the possibility of increasing the synchrotron radiation brightness. During machine studies the strengths of the quadrupoles adjacent to sextupoles were adjusted in order to compensate for the sextupole gradients and correct the large distortions in the dispersion shown in figure 5. The dispersion correction alone reduced the horizontal emittance from 110 nm*rad to 70 nm*rad. A new ring lattice is now (Autumn 1995) being commissioned which will further reduce the emittance to 50 nm*rad. The understanding of the rotational alignment of the X-Ray elements has also been used to improve the vertical beam size correction program.

IV. Acknowledgements

I would like to thank Jeff Corbett, Sam Krinsky, Martin Lee, and Dave Robin for stimulating discussions. Susila Ramamoorthy's improved fast averaged orbit readings helped provide the accurate orbit measurements necessary for the NSLS X-Ray Ring work. John Smith's help providing cpu time for the lengthy calculations was appreciated, as was Yong Tang's help integrating the program with the NSLS control system. Thanks to Lorraine Solomon, Eric Blum, Jeff Corbett, Glenn Decker, Sam Krinsky and Martin Lee for editing comments.

References

[1] E. Courant and H. Snyder, Ann. Physics, 3, p. 1-48 (1958).

[2] L. Emery, APS On-line Log Book, Argonne National Laboratory (April 21, 1995).

[3] J. Bengtsson and M. Meddahi, CPB Technical Note 003, Lawrence Berkeley Laboratory (1993).

[4] P.L. Morton, J.-L. Pellegrin, T. Raubenheimer, L. Rivkin, M. Ross, R.D. Ruth and W.L. Spence, Proc. 1985 IEEE Particle Accelerator Conference, 2291 (1985).

[5] P.L. Morton, J.-L. Pellegrin, T. Raubenheimer and M. Ross, Proc. 1987 IEEE Particle Accelerator Conference, 1367 (1987).

[6] J. Borer, A. Hofmann, J-P. Koutchouk, T. Risselada and B. Zotter, Proc. 1983 IEEE Particle Accelerator Conference, 2406 (1983).

[7] J. Borer, C. Bovet, A. Burns and G. Morpurgo, Proc. 1992 European Particle Accelerator Conference, 1082 (1992).

[8] P. Castro,J. Borer, A. Burns, G. Morpurgo and R. Schmidt, Proc. 1993 IEEE Particle Accelerator Conference, 2103 (1993).

[9] H. Grote,F.C. Iselin, The MAD Program, Version 8.1, CERN/SL/90-13, June 17, 1991.

[10] M.H.R. Donald, C. Blocker,A.W. Chao, R.J. Hollebeek, M.J. Lee, J.E. Linstadt, J.L. Siegrist, N. Spencer, Proc. 1981 IEEE Particle Accelerator Conference, 2207 (1981)

[11] M.J. Lee, Y. Zambre, W.J. Corbett, SLAC-PUB-5701A, 1991.

[12] W.J. Corbett, M.J. Lee and V. Ziemann, SLAC-PUB-6111, May, 1993.

[13] J. Safranek and M.J. Lee, AIP Conference Proceedings, Vol 315, 1993.

[14] Y. Chung, G. Decker and K. Evans, Proc. 1993 IEEE Particle Accelerator Conference, (1993)

[15] J. Bengtsson and M. Meddahi, Proc. 1994 European Particle Accelerator Conference, pg 1021.

[16] J. Safranek, Proc. 1995 IEEE Particle Accelerator Conference, (1995)

[17] S. Kamada, Proceedings of the Workshop on Non Linear Dynamics in Particle Accelerators, 1994.

[18] R. Biscardi and J.W. Bittner, 1989 IEEE Particle Acclerator Conference, pg 1516.